

Article

Theoretical Study on the Diels–Alder Reaction of Fullerenes: Analysis of Isomerism, Aromaticity, and Solvation

Diogo J. L. Rodrigues¹, Luís M. N. B. F. Santos¹ , André Melo² and Carlos F. R. A. C. Lima^{1,*} 

¹ Centro de Investigação em Química da Universidade do Porto, Department of Chemistry and Biochemistry, Faculty of Science, Institute of Molecular Sciences (IMS), University of Porto, Rua do Campo Alegre, P4169-007 Porto, Portugal

² Laboratório Associado para a Química Verde-REQUIMTE, Department of Chemistry and Biochemistry, Faculty of Science, University of Porto, Rua do Campo Alegre, P4169-007 Porto, Portugal

* Correspondence: carlos.lima@fc.up.pt

Abstract: Fullerenes are reactive as dienophiles in Diels–Alder reactions. Their distinctive molecular shape and properties result in interesting and sometimes elusive reaction patterns. Herein, to contribute to the understanding of fullerene reactivity, we evaluate the energies of reactions for Diels–Alder cycloadditions of C₆₀, C₇₀, and IC₆₀MA with anthracene (Ant), by means of DFT computational analysis in vacuum and solution. The methods used showed little differentiation between the reactivity of the different fullerenes. The C₇₀-Ant adducts where addition takes place near the edge of the fullerene were found to be the most stable regioisomers. For the IC₆₀MA-Ant adducts, the calculated energies of reaction increase in the order: equatorial > *trans*-3 > *trans*-2 ≈ *trans*-4 ≈ *trans*-1 > *cis*-3 > *cis*-2. The change in the functional suggests the existence of stabilizing dispersive interactions between the surface of the fullerene and the addends. HOMA (harmonic oscillator model of aromaticity) analysis indicated an increase in aromaticity in the fullerene hexagons adjacent to the bonded addend. This increase is bigger in the rings of bisadduct isomers that are simultaneously adjacent to both addends, which helps explain the extra stability of the equatorial isomers. Solvation by *m*-xylene decreases the exothermicity of the reactions studied but has little distinguishing effect on the possible isomers. Thermal corrections reduce the exothermicity of the reactions by ~10 kJ·mol⁻¹.

Keywords: fullerenes; ICMA; cycloaddition; regioisomers; DFT



Citation: Rodrigues, D.J.L.; Santos, L.M.N.B.F.; Melo, A.; Lima, C.F.R.A.C. Theoretical Study on the Diels–Alder Reaction of Fullerenes: Analysis of Isomerism, Aromaticity, and Solvation. *Organics* **2022**, *3*, 364–379. <https://doi.org/10.3390/org3040025>

Academic Editor: Edward Lee-Ruff

Received: 6 August 2022

Accepted: 19 September 2022

Published: 22 September 2022

Publisher's Note: MDPI stays neutral with regard to jurisdictional claims in published maps and institutional affiliations.



Copyright: © 2022 by the authors. Licensee MDPI, Basel, Switzerland. This article is an open access article distributed under the terms and conditions of the Creative Commons Attribution (CC BY) license (<https://creativecommons.org/licenses/by/4.0/>).

1. Introduction

Fullerenes are allotropes of carbon, consisting of sp^2 hybridized carbon atoms connected by single and double bonds, forming closed or partially closed surface(s) composed of five- and six-membered rings [1–3]. In C₆₀, the most famous fullerene [3], there exist only two types of bonds—[5,6] and [6,6] bonds. [5,6] bonds are at the junction of a pentagon and a hexagon (1.449 Å), and [6,6] bonds have a higher double bond character at the junction of two hexagons (1.391 Å) [2]. C₆₀ has low electron delocalization and is not fully aromatic. Double bonds in the pentagons would increase the strain in the molecule; hence the predominant resonant structure is the one with double bonds on the [6,6] bonds (between two hexagons) [3,4]. C₆₀ is a truncated icosahedron and has icosahedral symmetry (I_h)—the highest symmetry possible in a molecule—with a rotational symmetry number, σ_{sym} , of 60. Another important fullerene is C₇₀, with a structure similar to C₆₀ but with 70 carbon atoms, 25 hexagons, and 12 pentagons [5]. In relation to the C₆₀, it has an extra five hexagons inserted at the equator. This results in a large difference in chemical properties, especially since the resonance structure is altered. The molecule of C₇₀ has a D_{5h} symmetrical “egg-shaped” structure, with $\sigma_{\text{sym}} = 10$ [5].

The functionalization of fullerenes is the process of adding different functional groups to the fullerene structure via chemical reactions. Fullerene functionalization is a versatile tool to tune the physical and chemical properties of the fullerenes to better suit the desired

applications. For example, fullerenes can be made lipophilic, hydrophilic, and even amphiphilic, increasing their solubility in certain desired solvents [1,6]. Fullerenes and their derivatives have the chemistry of electron-deficient alkenes [2]. They have conjugated π systems that, unlike planar aromatic molecules, contain no hydrogens. Thus, their reactivity does not follow the same rules as classic aromatic molecules. Fullerenes can undergo redox reactions; they can participate in addition reactions; they can act as dienophiles and therefore react via a Diels–Alder cycloaddition with conjugated dienes (e.g., indene, tetracene, and anthracene). In Diels–Alder reactions, the diene binds to the [6,6] carbons of the fullerene, which are excellent dienophiles [1,2,4]. Fullerenes are highly strained molecules, and thus one important driving force in cycloaddition reactions to fullerenes is strain relief when the carbons go from sp^2 to sp^3 hybridization. These reactions are usually exergonic and exothermic. The limiting problem in the experimental studies of fullerene reactivity is their low solubility on most solvents [1,2,7].

In C_{70} , there are four different types of [6,6] bonds, as opposed to only one in C_{60} , which yields several isomers in the monoadduct resultant of the Diels–Alder reaction [1,8]. The stability of the different possible isomers can be evaluated based on the local curvature of the bonds in which the addend connects. Curvature depends on the fullerene size and on the distribution of hexagons and pentagons on the surface. In C_{60} , every [6,6] bond (30 in total) is of the α type (Figure 1a), but in C_{70} , there are ten α and ten β bond types. The α type bond is the most curved and thus most reactive, followed by the β type. The other two [6,6] bond types in C_{70} (the ones on the equatorial belt of hexagons) are lowly curved and are part of a local aromatic character zone, being far less reactive [9].

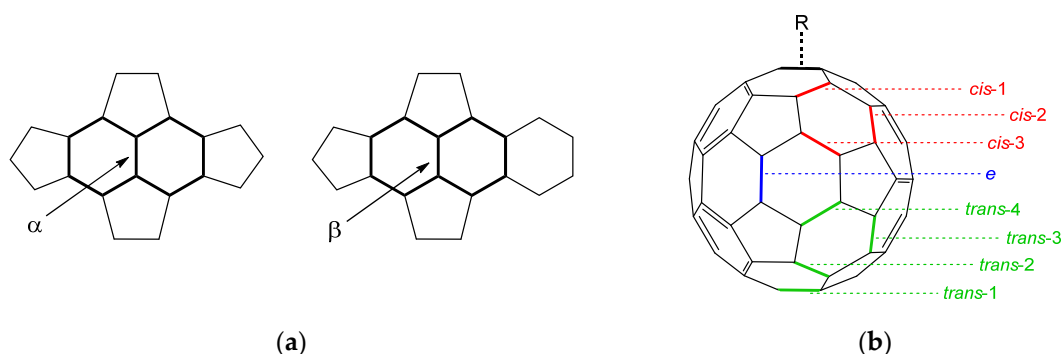


Figure 1. Bond nomenclature in fullerenes: (a) The two most curved and reactive [6,6] bonds in fullerenes; adapted from Thilgen et al. [9]; (b) Possible isomers for C_{60} bisadducts depending on the positions of the two groups; adapted from Ref. [1], nomenclature as suggested by Hirsch et al. [10].

After the first addition, subsequent additions can occur on the fullerene structure. In this scenario, the [6,6] bonds that used to be identical now have different reactivities, and thus several different possible isomers arise. In C_{60} , in theory, eight different isomers can be formed (Figure 1b), with a further splitting in different isomers for each if the addends are not symmetrical along the respective [6,6] bond axis [1]. Fullerene bisadducts have diverse applications due to their three-dimensional structures, with a wide variety of possible addend groups. Some applications occur in biology and advanced materials [1].

The functionalization of fullerenes by Diels–Alder reactions is a common procedure [1,5,7,11–15]. Sarova et al. studied the kinetics of Diels–Alder addition between C_{60} and anthracene and tetracene in the temperature range 22–62 °C, using UV-Vis spectroscopy [12]. For the concentrations used, they found only the presence of a monoadduct with both acenes. Wang et al. studied the cycloaddition of dimethylanthracene to endohedral fullerenes $^3\text{He}@C_{60}$ and $^3\text{He}@C_{70}$ via ^3He NMR spectroscopy in the temperature range of 22–52 °C [13]. They found the presence of the monoadduct and a bisadduct with six isomers in C_{60} , a monoadduct with a single relevant isomer, and a bisadduct with three isomers in C_{70} . Their results indicate that the first addition is thermodynamically more favorable in solution than the addition of a second adduct on the

fullerene for both fullerenes studied. Several fullerene adducts have been recognized as valuable electron transport materials for application in organic semiconductor devices, with particular relevance in organic photovoltaics [16–21]. Some well-known examples include the commercially available IC₆₀MA (indene C₆₀ mono adduct) and IC₆₀BA (indene C₆₀ bis adduct) [16,20], and also the analogous C₇₀ compounds, IC₇₀MA and IC₇₀BA [16,21].

The analysis of fullerene reactivity as dienophiles in Diels–Alder cycloadditions has been investigated both experimentally and theoretically [1,2,4,22–28]. The pioneering computational work of Fujimoto and co-workers suggested that the double addition of butadiene to C₆₀ is not highly regioselective [22]. Solà et al. theoretically compared the reactivity of C₆₀ and C₇₀ with butadiene [23]. The authors found that in the gas phase, C₇₀ seems slightly more reactive, but in toluene solvent, the effects reverse this order by significantly decreasing the energy barrier in the butadiene addition to C₆₀ [23]. As indicated in the comprehensive work of Li and co-workers on the separation of IC₆₀BA regioisomers, the conventional synthesis of IC₆₀BA yields no *cis*-isomers owing to steric hindrance [24]. The *trans*-2, *trans*-3, *trans*-4, and *e*- isomers of NC₆₀BA (dihydronaphthyl-based C₆₀ fullerene bisadduct) were isolated and used as acceptors for P3HT-based polymer solar cells (PSCs) [25]. The calculated relative stabilities of C₆₀ and C₇₀ bisadducts with anthracene suggest that the thermodynamic stability of the regioisomers decrease in the following order: *trans*-3 ≥ *e*- > *trans*-2 > *trans*-4 ≥ *trans*-1 > *cis*-3 > *cis*-2 [26].

In this work, we present a comprehensive computational evaluation of reaction thermodynamics for Diels–Alder cycloadditions with fullerenes, focusing on the effect of dienophile, solvation, and isomerism. For the three fullerenes shown in Figure 2a, C₆₀, C₇₀, and IC₆₀MA, we have calculated the energies at *T* = 0 K and enthalpies at *T* = 298.15 K for the Diels–Alder reaction with anthracene (Figure 2b) in a vacuum and in a solution of *m*-xylene. This includes a detailed analysis of all possible regioisomers. The calculations were performed using various DFT computational methods to study the effect of the basis-set and the inclusion of dispersion-corrected functionals. This work aims to contribute to the understating of the chemical reactivity of fullerenes, building on the computational knowledge of reaction thermodynamics in vacuum and solution.

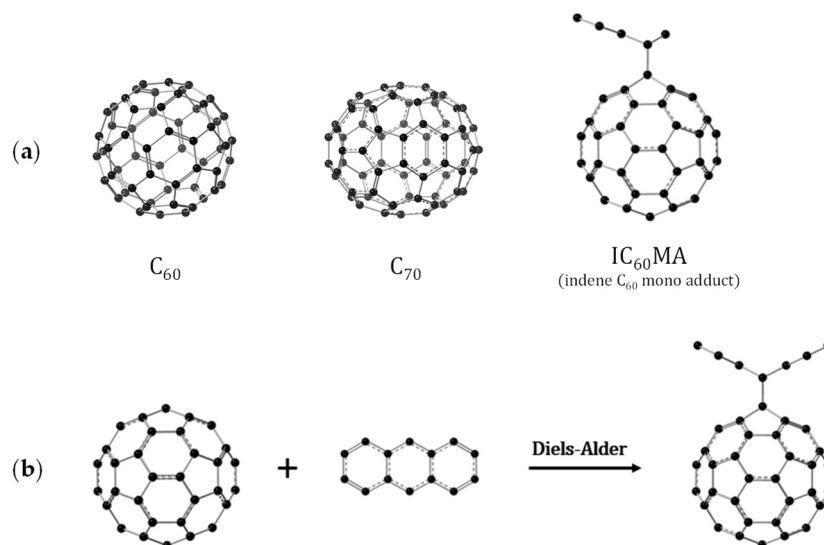


Figure 2. Schematic representation of: (a) The fullerenes studied in this work; (b) Diels–Alder reaction between the fullerenes and anthracene.

2. Materials and Methods

All of the quantum chemical calculations were performed using the Gaussian 09 software package [29]. For the molecules included in the computational study, full geometry optimizations, in a vacuum and without symmetry restrictions, were performed at the M06-2X/6-31+G(d) level of theory [30]. The M06-2X functional ensures that dispersive

interactions, which are important for correctly describing the systems under study (e.g., intramolecular interaction between the fullerene surface and the aromatic addend), are taken into account [31]. This functional has also shown good performance in describing supramolecular complexes that involve fullerenes [32]. Frequency calculations were performed at the same level for a few selected fullerenes—no imaginary frequencies were found, confirming that the structures correspond to true minima. Herein, we assume that the optimized geometries obtained for the fullerenes correspond to the absolute minimum structures of the molecules. Due to the low molecular flexibility of these fullerene molecules and the high symmetry of the C_{60} and C_{70} moieties, the potential energy surface should not contain structurally very different local minima. To better validate this assumption, additional optimizations were undertaken for the *trans-2 a* and *trans-2 b* regioisomers of $IC_{60}MA$, starting with different initial geometries—the energies and optimized geometries were found to be the same as before.

The energies of several Diels–Alder reactions of fullerenes were calculated in a vacuum and in solution. The geometry optimizations were performed under a vacuum for all molecules and isomers studied; for a few representative molecules, the geometry optimization was also performed in solution. The universal continuum solvation model based on density (SMD) [33] was used to calculate the electronic energies of the molecules in the solvent *m*-xylene using M06-2X/6-31+G(d). For the adducts of C_{70} and $IC_{60}MA$ with anthracene, all of the relevant isomers were explored; the geometry of each regioisomer was optimized individually. For some representative fullerenes, additional single-point energy calculations were performed on the M06-2X/6-31+G(d) optimized geometries at the following levels of theory: B3LYP/6-31+G(d) (effect of functional), M06-2X/6-311++G(2d,p) (effect of basis set), and MP2/cc-pVDZ (effect of theoretical method). Owing to the very high demand for computational resources, the MP2 calculations were only carried out for a limited set of molecules.

3. Results and Discussion

3.1. Optimized Molecular Structures and Isomers

The M06-2X/6-31+G(d) optimized molecular structures for the four distinguishable [6,6] isomers of $AC_{70}MA$ (anthracene C_{70} mono adduct) are shown in Figure 3. Isomer *a* has the anthracene addend bonded in the edge of the fullerene, where it is locally most similar to C_{60} , while isomer *d* has the anthracene bonded on the equatorial belt of C_{70} (in which it differs most from C_{60}). Thus, the structural similarity to C_{60} decreases from isomer *a* to *d*.

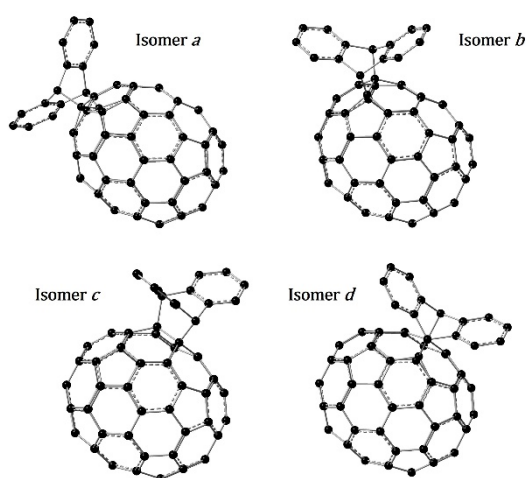


Figure 3. Optimized molecular structures for the four possible regioisomers of $AC_{70}MA$.

For $AIC_{60}BA$ (anthracene indene C_{60} bis adduct), of a total of 29 possible isomers, 14 regioisomers were optimized using M06-2X/6-31+G(d); the optimized molecular struc-

tures are shown in Figure 4. Nearly all of the regioisomers—except *trans*-1, *e*-face *a*, and *e*-face *b*—have a corresponding enantiomer. The four possible *cis*-1 isomers (two pairs of enantiomers) were not included in this study because they are clearly unstable due to the overlap of the addends, which generates very strong repulsive forces. Thus, their contribution to the isomer population and reaction equilibrium can be neglected. This adds up to 29 total isomers of AIC₆₀BA that correspond to the 29 possible bonds on which anthracene can add, 30 bonds in the C₆₀ structure minus the one in which indene is already bonded.

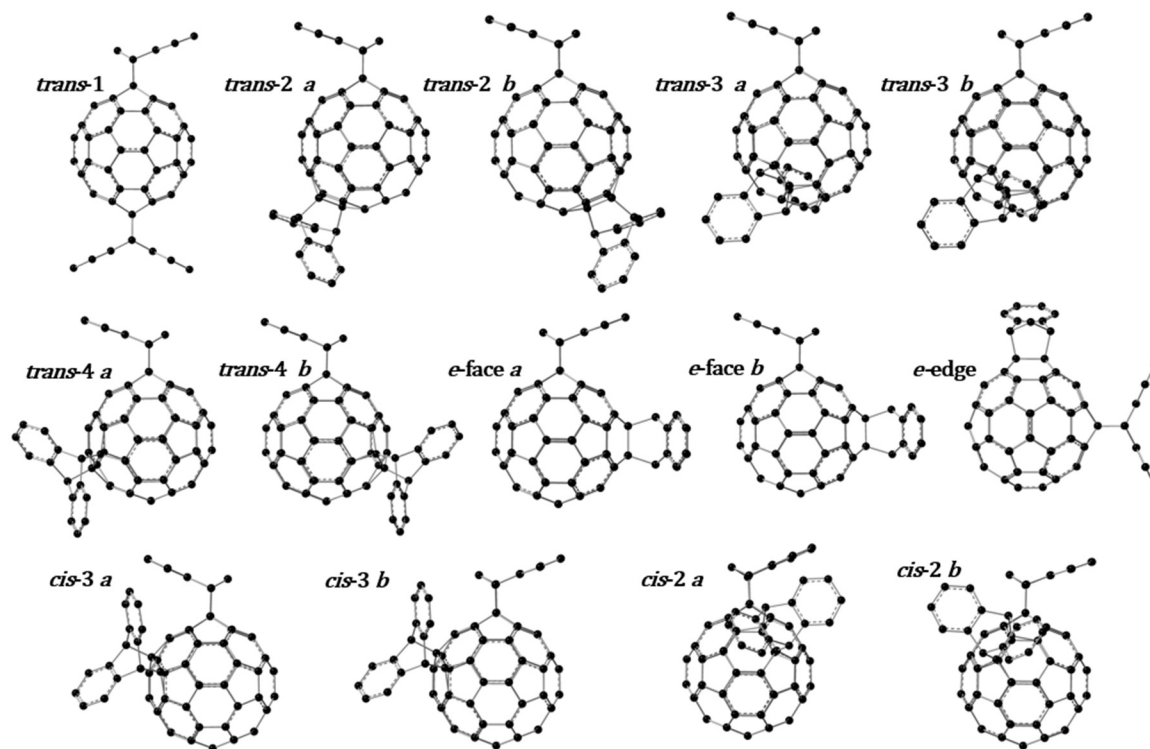


Figure 4. Optimized molecular structures for 14 regioisomers of AIC₆₀BA (IC₆₀MA adducts with anthracene); only the four *cis*-1 isomers were excluded from the computational study due to obvious steric repulsions. With exception of *trans*-1, *e*-face *a*, and *e*-face *b*, all the regioisomers presented have a corresponding enantiomer, making up a total of 29 isomers (if including the four *cis*-1).

3.2. Electronic Energies of Reaction in Vacuum

The complete theoretical analysis of the Diels–Alder reaction for the fullerenes studied, i.e., including all the meaningful regioisomers (see Figures 3 and 4), was undertaken at the M06-2X/6-31+G(d) level of theory. Additionally, single-point energy calculations in a vacuum were performed on a representative set of the M06-2X/6-31+G(d) optimized geometries using other computational methods: (i) B3LYP/6-31+G(d) to evaluate the effect of changing the DFT functional, and, in particular, to compare between functionals with and without empirical dispersion correction terms; (ii) M06-2X/6-31++G(2d,p) to evaluate the effect of improving on the basis set; and (iii) MP2/cc-pVDZ, and simultaneously HF/cc-pVDZ, to explore the use of ab initio quantum chemistry methods and the contribution of correlation energy for these Diels–Alder reactions. The calculations referred to in (i) and (ii) were made for the reactions involving the following representative set of fullerenes: AC₆₀MA, the two most stable regioisomers of AC₇₀MA (isomer *a* and isomer *b*), and four regioisomers of AIC₆₀BA (*trans*-1, *trans*-3 *a*, *e*-face *a*, and *cis*-2 *b*), which include the most stable *e*-face *a* regioisomer and different types of bisadducts (concerning the bond distance between the anthracene and indene groups). The reaction of C₆₀ with indene was also studied using all the DFT methods referred before to evaluate the differences in reactivity and stability due to changing the diene.

The calculated electronic energies of the reaction in a vacuum, at $T = 0$ K, $\Delta_r E_{el,m}$ (g, 0 K), for the Diels–Alder cycloadditions between the fullerenes studied with two dienes, indene (Ind) and anthracene (Ant), are presented in Table 1.

Table 1. Electronic energies of reaction in vacuum, at $T = 0$ K, for the Diels–Alder cycloadditions of the fullerenes studied with indene (Ind) and anthracene (Ant), calculated at various levels of theory; all geometries optimized using M06-2X/6-31+G(d)¹.

Reaction	$\Delta_r E_{el,m}$ (g, 0 K)/kJ·mol ^{−1}			
	M06-2X/ 6-31+G(d)	M06-2X/ 6-311++G(2d,p)	B3LYP/ 6-31+G(d)	MP2/ cc-pVDZ ²
R1. C ₆₀ + Ind → IC ₆₀ MA	−116.6	−106.4	−31.0	---
R2. C ₆₀ + Ant → AC ₆₀ MA	−95.4	−85.4	7.8	−165.5 (−30.2)
R3. C ₇₀ + Ant → AC ₇₀ MA				
<i>a</i>	−96.6	−86.4	8.2	---
<i>b</i>	−91.6	−80.4	20.9	---
<i>c</i>	−19.5	−9.2	---	---
<i>d</i>	95.5	105.6	---	---
R4. IC ₆₀ MA + Ant → AIC ₆₀ BA ³				
<i>trans</i> −1	−91.2	−81.1	14.6	---
<i>trans</i> −2 <i>a</i>	−91.9	---	---	---
<i>trans</i> −2 <i>b</i>	−92.1	---	---	---
<i>trans</i> −3 <i>a</i>	−95.9	−86.1	8.6	---
<i>trans</i> −3 <i>b</i>	−95.0	---	---	---
<i>trans</i> −4 <i>a</i>	−91.3	---	---	---
<i>trans</i> −4 <i>b</i>	−91.2	---	---	---
<i>e</i> -face <i>a</i>	−96.5	−86.3	9.3	---
<i>e</i> -face <i>b</i>	−96.1	---	---	---
<i>e</i> -edge	−96.1	---	---	---
<i>cis</i> −3 <i>a</i>	−79.9	---	---	---
<i>cis</i> −3 <i>b</i>	−79.7	---	---	---
<i>cis</i> −2 <i>a</i>	−64.9	---	---	---
<i>cis</i> −2 <i>b</i>	−77.9	−67.8	32.6	---

¹ The optimized molecular structures of the fullerenes are shown in Figures 3 and 4. For the other methods other than M06-2X/6-31+G(d), the calculations (single-point energy) were performed for some representative cases only. ² The HF/cc-pVDZ result is shown in parenthesis. ³ The AIC₆₀BA regioisomers are ordered up-to-down by increasing proximity of Ant from Ind.

Concerning the two dienes, Ind and Ant, the results are not surprising in indicating that the reaction with Ind is more exothermic than with Ant. This agrees with the greater reactivity of Ind as a diene in Diels–Alder cycloadditions [34]. The reactions of the three dienophiles, C₆₀, C₇₀, and IC₆₀MA with Ant, show similar $\Delta_r E_{el,m}$ (g, 0 K), considering the most stable regioisomers of AC₇₀MA (*isomer a*) and AIC₆₀BA (*e*-face *a*). Thus, our computational study does not predict a significant difference in reactivity, due to electronic structure (which is the most significant contribution to the enthalpy of the reactions), between the three fullerenes when reacting with Ant.

For C₇₀, the comparison between the regioisomers clearly reveals an increasing tendency for reaction, more negative $\Delta_r E_{el,m}$ (g, 0 K), as the [6,6] additions occur closer to the edges of the fullerene, where it is more similar to C₆₀ in local curvature and bond length. This is also well understood by inspecting the type of [6,6] bonds to where the diene binds. In *isomer a*, it binds to an α type and in *isomer b* to a β type bond (see Figure 1a). The much higher (more positive) values of $\Delta_r E_{el,m}$ (g, 0 K) for *isomers c* and *d* are easily explained by noting that these [6,6] bonds, contrary to α and β types, are not linked to two pentagons. In *isomer c*, it is linked to one pentagon and in *d* to none (the [6,6] bond is surrounded by four hexagons). This bond topology in C₇₀ is very impactful on reaction energetics, making the reaction for *isomer d* energetically very disfavored.

For the reaction of IC₆₀MA with Ant, three groups of regioisomers can be discerned. The *cis*-isomers are clearly the least stable, which probably arises from steric repulsions between the two addends. Note that the most unstable regioisomer is *cis*-2 *a*, which is the one (excluding the *cis*-1 isomers) where the addends have a more notorious overlap of

electron density. The *trans*- and equatorial regioisomers fall into two categories of energetic stability. They all have similar energies and thus significant populations at equilibrium, and all should be considered as relevant products in Diels–Alder cycloadditions. The three *e*- isomers, *trans*-3 *a*, and *trans* 3 *b* stand out as the most stable in the set. Among these five, the differences in $\Delta_r E_{el,m}$ (g, 0 K) are so small they can be neglected, and no isomer deserves to be clearly distinguished as the most stable. The remaining *trans*-regioisomers (1, 2 *a*, 2 *b*, 4 *a*, and 4 *b*) are slightly less stable. Our computational results are in good agreement with the literature concerning both the little differentiation between dienophiles [22,23] and the ordering in reactivity [24–26].

In fullerenes, reactivity is closely related to double-bond character and curvature; usually, the most reactive bonds are shorter and have higher local curvature [2,4]. Although bond length can be a good predictor of reactivity (here, we speak of reactivity in the context of reaction kinetics), its implications on reaction thermodynamics are questionable. In C₇₀, there is a qualitative relation between the calculated bond lengths and $\Delta_r E_{el,m}$ (g, 0 K) for the reaction with Ant. The lengths of the bonds in C₇₀, in Å, to which Ant binds increase in the order: isomer *b* (1.380) < isomer *a* (1.390) < isomer *c* (1.416) < isomer *d* (1.470), which approximately follows the increase (more positive value) in $\Delta_r E_{el,m}$ (g, 0 K). In IC₆₀MA, the bonds leading to the more stable *e*- regioisomers are, in fact, slightly shorter than those leading to the *trans*- (≈ 1.387 Å vs ≈ 1.389 Å, respectively). On the other hand, the trend in $\Delta_r E_{el,m}$ (g, 0 K) among the *trans*-isomers has no apparent relation to the calculated bond lengths.

This work is more focused on the thermodynamics of Diels–Alder reactions than on the kinetic reactivity (for which bond length could be a better descriptor). Thermodynamic analysis requires knowledge of both reactants and products. In this way, and given that in this analysis, the reactants are the same, it makes more sense to compare the products (i.e., the AC₇₀MA and AIC₆₀BA regioisomers). The trend for AC₇₀MA highlights the contribution from the local curvature of the fullerene and aromaticity for reaction energetics. $\Delta_r E_{el,m}$ (g, 0 K) is more negative for those isomers in which Ant binds to a bond with greater local curvature. Isomers *a* and *b* show greater local curvature (similar to C₆₀), but for isomers *c* and *d*, the reactive zone is more planar. Curvature is intrinsically related to bond strain, with greater curvature being associated with the release of more strain energy upon binding to the diene [2,4,9]. The question of aromaticity in fullerenes is still controversial, but some authors advocate that, contrary to the non-aromatic pentagons, the hexagons can be slightly aromatic [35,36]. By this reasoning, the formation of the least stable AC₇₀MA isomers, *c* and *d*, implies the disruption of aromaticity in three and four hexagons, respectively, while in isomers, *a* and *b*, only two hexagons are sacrificed. The differentiation between *trans*- and *e*- isomers in AIC₆₀BA, however, is harder to rationalize. All isomers are close in energy, and bond topology in the C₆₀ framework is less diverse than in C₇₀ [9]. We investigated the possibility that, after the binding of the diene, the four adjacent hexagons (not those directly bonded) become more aromatic. This makes sense, considering that the release of strain upon addition allows for some geometry adjustment of the surrounding fullerene surface [35]. A quick inspection of the IC₆₀MA and AC₆₀MA optimized structures supports this hypothesis, with the four hexagons adjacent to the addend (see Figure 5) showing more aromatic character, as suggested by shorter bonds (on average) and smaller bond-length alteration, in comparison to C₆₀. Following this reasoning, we employed the Harmonic Oscillator Model of Aromaticity (HOMA) [37,38] on the fullerenes to gain some insight into the aromatic character of the relevant hexagons. The bond lengths used in the calculation of HOMA indices were taken from the M06-2X optimized structures. HOMA indices were calculated using the refined model of HOMA [39]:

$$\text{HOMA} = 1 - [\alpha(r_{\text{opt}} - r_{\text{av}})^2 + \alpha/n \cdot \sum (r_{\text{av}} - r_i)^2] = 1 - \text{EN} - \text{GEO} \quad (1)$$

where *n* is the number of bonds considered in the summation (*n* = 6 for the case of fullerene hexagons), r_{opt} stands for the optimal value of a specific bond length in a fully aromatic system (for CC bonds $r_{\text{opt}} = 1.388$ Å) [38], r_{av} is the average bond length of the *n* bonds,

r_i is the bond length of bond i , and $\alpha = 257.7 \text{ \AA}^{-2}$ is a normalization constant. The term EN is closely related to de-aromatization due to bond energies, and GEO is attributed to de-aromatization due to geometric contributions, namely bond length alternation.

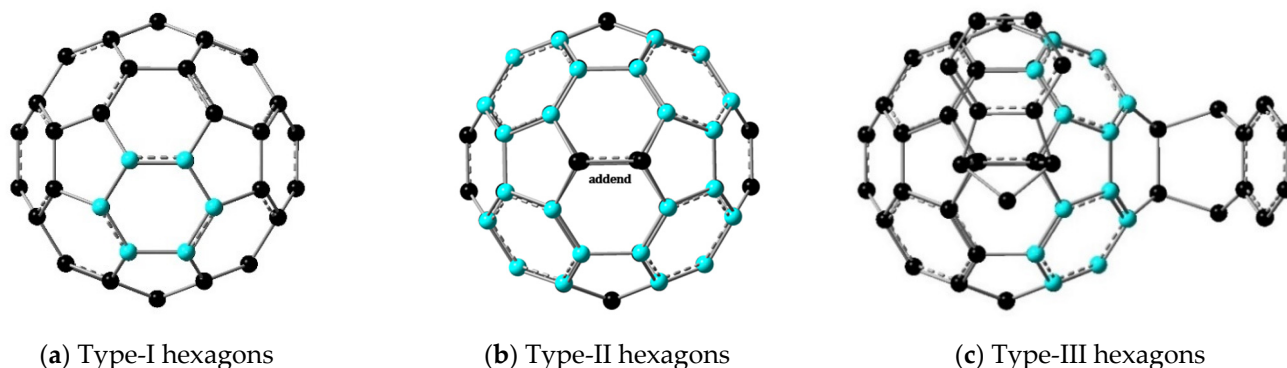


Figure 5. Schematic view of the three types of hexagons considered in the HOMA analysis (in blue): (a) regular hexagons in C_{60} ; (b) and (c) adjacent hexagons to the addends in fullerene adducts, which, due to release of bond strain, become more aromatic. In the case of (c), they are simultaneously adjacent to two addends. Structures taken from the optimized M06-2X/6-31+G(d) geometries.

In our HOMA analysis, we have distinguished between three types of hexagons (see Figure 5): Type-I (those not adjacent to an addend, similar to all hexagons in C_{60}), Type-II (the four hexagons adjacent to an addend), and Type-III (the superposition of two Type-II hexagons). This distinction is based on the different bond topology and calculated HOMA indices, which increase (higher aromaticity) in the order: Type-I < Type-II < Type-III. The detailed results of our HOMA analysis are presented in Table 2. In C_{70} , there are three types of hexagons: Ia, the hexagons in the edges of C_{70} ; Ic, the hexagons in the center of the equatorial belt of C_{70} ; and Ib, the rings adjacent to Ic in the equatorial belt (see Figure S1 for a visual display). This gives rise to three different Type-II rings in C_{70} adducts: IIa, IIb, and IIc.

Table 2 shows the average HOMA results for each type of hexagon in the fullerenes studied; the detailed results for each individual hexagon are presented as Supplementary Materials. We chose to present the average values for a question of simplicity, and because the HOMA values do not vary significantly within the same type of hexagon. Furthermore, it is noteworthy that the addition of the addend only alters the aromaticity of the four adjacent hexagons; all the others remain similar to the Type-I hexagons in the parent C_{60} or C_{70} . The results reveal a clear gain in aromaticity in the four hexagons adjacent to the adduct; in the C_{60} adducts, HOMA increases from ~ 0.2 (Type-I) to 0.4–0.5 (Type-II). This increase in aromaticity is manifested by a decrease in both the EN and GEO parameters, although according to HOMA, de-aromatization in fullerenes has a stronger contribution from bond length alternation. In the case of the bisadducts, the aromaticity gain is even larger if the ring is simultaneously adjacent to both addends (Type-III), in which case the HOMA value is ~ 0.7 . All three equatorial isomers of $AIC_{60}BA$ have two such hexagons, which can help explain their higher stability. However, aromaticity changes do not seem enough to explain the relative stability of *trans*-3 isomers, which remains to be explained. The same trend upon addend addition is observed in C_{70} . Although aromaticity contributes to $\Delta_r E_{el,m}$, the differentiation between $AC_{70}MA$ isomers *a* and *b* is better explained by bond curvature and release of strain. The gain in aromaticity upon addition probably contributes to the exothermicity of Diels–Alder reactions with fullerenes. According to our HOMA analysis, and as previously reported in the literature [35,40,41], the energetic stability of similar hexakis adducts of C_{60} will probably benefit from all adjacent hexagons (a total of eight) being Type-III (in fact, these rings can be even more aromatic than Type-III because they result from the superposition of three Type-II hexagons). Another important remark is the difference in aromaticity found for C_{70} hexagons—while the aromaticity of Type-Ia

edge hexagons seems comparable to the C_{60} hexagons—Type-Ic equatorial hexagons have a much higher HOMA value. On the contrary, Type-Ib hexagons (adjacent to Type-Ic) are probably slightly anti-aromatic.

Table 2. HOMA analysis of aromaticity, including the average EN and GEO values, for the hexagons in fullerenes and hexagons adjacent to the addend in the respective adducts. The average values were calculated by averaging over all adjacent rings of the same type.

Molecule	<EN>	<GEO>	<HOMA>	Hexagon Type (Qty.) ¹
C_{60} ²	0.267	0.529	0.204	I (20)
C_{70}	0.219	0.462	0.319	Ia (10)
	0.473	0.705	−0.177	Ib (10)
	0.253	0.259	0.489	Ic (5)
IC ₆₀ MA	0.162	0.366	0.471	II (4)
AC ₆₀ MA ³	0.158	0.368	0.474	II (4)
AC ₇₀ MA isomer <i>a</i>	0.126	0.299	0.575	IIa (2)
	0.330	0.585	0.085	IIb (2)
AC ₇₀ MA isomer <i>b</i>	0.118	0.306	0.576	IIa (2)
	0.178	0.199	0.624	IIc (2)
AIC ₆₀ BA <i>trans</i> −1	0.160	0.354	0.486	II (8)
AIC ₆₀ BA <i>trans</i> −2 <i>a</i>	0.163	0.363	0.474	II (8)
AIC ₆₀ BA <i>trans</i> −2 <i>b</i>	0.163	0.363	0.474	II (8)
AIC ₆₀ BA <i>trans</i> −3 <i>a</i>	0.168	0.368	0.464	II (8)
AIC ₆₀ BA <i>trans</i> −3 <i>b</i>	0.167	0.367	0.465	II (8)
AIC ₆₀ BA <i>trans</i> −4 <i>a</i>	0.080	0.217	0.703	III (1)
	0.163	0.369	0.468	II (6)
AIC ₆₀ BA <i>trans</i> −4 <i>b</i>	0.083	0.228	0.690	III (1)
	0.166	0.377	0.457	II (6)
AIC ₆₀ BA <i>e</i> -face <i>a</i>	0.084	0.222	0.694	III (2)
	0.158	0.356	0.486	II (4)
AIC ₆₀ BA <i>e</i> -face <i>b</i>	0.086	0.232	0.682	III (2)
	0.160	0.356	0.484	II (4)
AIC ₆₀ BA <i>e</i> -edge	0.085	0.226	0.689	III (2)
	0.159	0.358	0.483	II (4)

¹ Type of hexagon and quantity of each type. ² All 20 hexagons are equivalent. ³ All four hexagons adjacent to the addend are equivalent.

3.3. Effect of Computational Method and Basis-Set

Next, we analyze the effect of the computational method on the calculated reaction energies (see Table 1). When compared to the dispersion-corrected M06-2X, the B3LYP functional predicts the fullerenes to be much less reactive towards Diels–Alder addition. In fact, Solà and co-workers have shown that the inclusion of dispersion corrections is essential for the study of the chemical reactivity of fullerenes [42,43]. Moreover, as verified experimentally [12–15], these reactions are significantly exothermic, thus proving that M06-2X describes energetics better. A great fraction of the B3LYP destabilization is due to the inability of this functional to describe London dispersion forces. B3LYP probably “sees” the interaction between the Ant “wings” with the fullerene surface as highly repulsive. Interestingly, the differences, Δ , between the values of $\Delta_r E_{el,m}$ (g, 0 K) calculated using M06-2X and B3LYP (both with 6-31+G(d)) nicely support this reasoning. The smallest difference is observed for R1 ($\Delta = 86 \text{ kJ}\cdot\text{mol}^{-1}$), the reaction with Ind, which is smaller than Ant and has only one “wing” to overlap with the C_{60} surface. For the two AC₇₀MA isomers, Δ is greater for isomer *b* (113 as compared to 105 $\text{kJ}\cdot\text{mol}^{-1}$ for isomer *a*). Moreover,

for isomer *a*, Δ is similar to three representative isomers of AIC₆₀BA (*trans*-1, *trans*-3 *a*, and *e*-face *a*); for *cis*-2 *b* Δ is slightly larger. This is easily understood by recalling that in isomer *a* of AC₇₀MA, Ant binds to the place where the local curvature is more similar to C₆₀. In isomer *b* of AC₇₀MA, Δ is larger because one “wing” of Ant overlaps with the flatter surface of C₇₀ closer to the equatorial belt of hexagons. In the *cis*-2 *b* isomer of AIC₆₀BA, Δ is larger because there is an additional intramolecular contact between the two addends.

If using M06-2X with a larger basis set, 6-311++G(2d,p), a less negative $\Delta_r E_{el,m}$ (g, 0 K) was found for all fullerenes studied. It is known that using a more complete basis set lowers the energy of a molecular species, approximating it to the variational limit (the calculated electronic energies for each species are compiled in the Supplementary Materials). However, the electronic energies were lowered more in favor of the reactants, making the reactions less favorable. The differences between the two basis sets are very constant for all reactions ($\Delta \approx 10 \text{ kJ}\cdot\text{mol}^{-1}$). One possible contribution to this difference is the smaller basis set superposition error (BSSE) if using the larger 6-311++G(2d,p) basis [44]. The stabilizing interaction between the fullerene surface and the addend in adduct molecules is probably overestimated to a larger extent, due to BSSE, by the smaller 6-31+G(d). The MP2/cc-pVDZ result for R2 corroborates the importance of correlation energy in the fullerenes, with the uncorrelated Hartree-Fock (HF) predicting a substantially less negative $\Delta_r E_{el,m}$ (g, 0 K). This correlation is manifested in both electronic conjugation effects and London dispersive interactions, although MP2/cc-pVDZ probably overestimates the correlation energy.

Together, these results highlight the importance of intramolecular interactions with a significant contribution from London dispersion, such as $\pi\cdots\pi$ interactions involving the aromatic addends at the surface of the fullerene.

3.4. Solvation Energies in *m*-Xylene. Enthalpies of Reaction at $T = 298.15 \text{ K}$

The optimized M06-2X/6-31+G(d) geometries in a vacuum were used to calculate the electronic energies of solvation, $\Delta_{solv} E_{el,m}$ (*m*-xylene) for each species using SMD [33]. To economize the computational resources, the geometries were not reoptimized in solution, except for a few representative cases. Given the relatively low flexibility of the molecules studied (e.g., they do not possess low-frequency vibrational modes such as those associated to internal rotation) and the absence of any obvious conformational equilibria, we assume that the preferred geometry in the weakly polar *m*-xylene shall not be significantly different from that in the gas phase. In fact, for those molecules that were reoptimized in a solution of *m*-xylene using SMD, the calculated electronic energies show variations smaller than $1 \text{ kJ}\cdot\text{mol}^{-1}$, thus supporting our assumption (details in the Supplementary Materials). The calculated $\Delta_{solv} E_{el,m}$ (*m*-xylene) for all the molecules studied are presented in Table 3. The results follow the expected trend, with $\Delta_{solv} E_{el,m}$ (*m*-xylene) becoming more negative as the molecular surface area increases. There are only slight differences between regioisomers; however, this can alter the order of reactivity if going from gas to solution. To analyze the effect of solvation on the Diels–Alder reactions, we calculated the energies of reaction in solution, $\Delta_r E_{el,m}$ (*m*-xylene), and the results are presented in Table 4. The inclusion of solvation makes $\Delta_r E_{el,m}$ less negative, meaning that *m*-xylene solvates the reagents better than the products. This makes sense, considering the stoichiometry of the reactions and the smaller total surface area of the product in comparison to the sum of the two reactants. The effect of solvation is most pronounced in R2 (C₆₀ + Ant reaction) and less pronounced in R1 (C₆₀ + Ind), although this differentiation among reactions is very faint. The trend in $\Delta_r E_{el,m}$ for the reactions of the three dienophiles (C₆₀, C₇₀, and IC₆₀MA), considering the most stable isomers, is tenuous both in a vacuum and in *m*-xylene. However, solvation makes it slightly more noticeable in the order of more negative $\Delta_{solv} E_{el,m}$: C₆₀ < C₇₀ < IC₆₀MA. In the regioisomers of AIC₆₀BA, the effect of solvation also shows a small dependence on the addends' position, slightly favoring the *e*-edge isomer. In short, solvation by *m*-xylene, as simulated by SMD, makes the reaction $\approx 20 \text{ kJ}\cdot\text{mol}^{-1}$ less exothermic, but this effect is almost independent of the dienophile, diene, and position of the addends.

Table 3. Electronic energies of solvation in *m*-xylene, at $T = 0$ K, for the compounds involved in the Diels–Alder cycloadditions of the fullerenes studied, calculated as M06-2X/6-31+G(d) single-point energy calculations on the M06-2X/6-31+G(d) optimized geometries in vacuum and as M06-2X/6-31+G(d) geometry optimizations in *m*-xylene solution (shown in parenthesis).

Molecule	$\Delta_{\text{solv}}E_{\text{el,m}}(m\text{-xylene})/\text{kJ}\cdot\text{mol}^{-1}$
Ind	−29.7 (−29.8)
Ant	−42.3 (−42.3)
C ₆₀	−145.3 (−146.0)
C ₇₀	−164.2 (−164.6)
IC ₆₀ MA	−157.3 (−157.4)
AC ₆₀ MA	−166.1 (−166.2)
AC ₇₀ MA	
<i>a</i>	−186.4
<i>b</i>	−187.0 (−187.0)
AIC ₆₀ BA ¹	
<i>trans</i> −1	−179.9
<i>trans</i> −2 <i>a</i>	−180.8
<i>trans</i> −2 <i>b</i>	−180.3
<i>trans</i> −3 <i>a</i>	−180.8
<i>trans</i> −3 <i>b</i>	−180.4
<i>trans</i> −4 <i>a</i>	−179.4
<i>trans</i> −4 <i>b</i>	−179.1
<i>e</i> -face <i>a</i>	−180.2 (−180.3)
<i>e</i> -face <i>b</i>	−179.6
<i>e</i> -edge	−181.4
<i>cis</i> −3 <i>a</i>	−178.8
<i>cis</i> −3 <i>b</i>	−180.7
<i>cis</i> −2 <i>a</i>	−178.5
<i>cis</i> −2 <i>b</i>	−180.0

¹ The AIC₆₀BA regioisomers are ordered up-to-down by increasing proximity of Ant from Ind.

The former analyses of $\Delta_r E_{\text{el,m}}$, at $T = 0$ K, ignore the contributions from ZPE and thermal enthalpy. In this work, we also pretend to report reasonable computational predictions of reaction thermodynamics under real experimental conditions. To this end, we have estimated the standard molar enthalpies of reaction in *m*-xylene, at $T = 298.15$ K, $\Delta_r H_{\text{m}}^0(m\text{-xylene}, 298.15\text{ K})$ using the following Equation:

$$\Delta_r H_{\text{m}}^0(m\text{-xylene}, 298.15\text{ K}) = \Delta_r E_{\text{el,m}}^{6-311++G(2d,p)}(\text{g}, 0\text{ K}) + \Delta\left(\Delta_{\text{solv}}E_{\text{el,m}}^{6-31+G(d)}\right) + \Delta_r H_{\text{thermal,m}}^{6-31+G(d)} \quad (2)$$

where $\Delta_r E_{\text{el,m}}^{6-311++G(2d,p)}(\text{g}, 0\text{ K})$ is the calculated electronic energy of reaction in a vacuum using M06-2X/6-311++G(2d,p) (Table 1), $\Delta\left(\Delta_{\text{solv}}E_{\text{el,m}}^{6-31+G(d)}\right)$ is the calculated solvation energy of the reaction using M06-2X/6-31+G(d) (Table 3, products minus reactants), and $\Delta_r H_{\text{thermal,m}}^{6-31+G(d)}$ is the thermal correction to enthalpy (including ZPE and thermal enthalpy from 0 K to 298.15 K), as obtained from the frequencies calculations using M06-2X/6-31+G(d). The term $\Delta_r H_{\text{thermal,m}}^{6-31+G(d)}$ was not corrected for scaling factors, which is a reasonable approximation considering that their contribution shall partially cancel out in the calculation of enthalpies of reaction. The results are presented in Table 4 for the selected representative reactions.

Table 4. Electronic energies of reaction in *m*-xylene, at $T = 0$ K, standard enthalpies of reaction in vacuum, at $T = 298.15$ K, and estimated standard enthalpies of reaction in *m*-xylene, at $T = 298.15$ K, for the Diels–Alder cycloadditions of the fullerenes studied with indene (Ind) and anthracene (Ant), calculated at the M06-2X/6-31+G(d) level of theory.

Reaction	$\Delta_r E_{el,m}$ (<i>m</i> -xylene) ¹ /kJ·mol ^{−1}	$\Delta_r H_m^0$ (g, 298.15 K)/kJ mol ^{−1}	$\Delta_r H_m^0$ (<i>m</i> -xylene, 298.15 K) ² /kJ mol ^{−1}
R1. C ₆₀ + Ind → IC ₆₀ MA	−98.8 (−98.2)	−105.4	−77
R2. C ₆₀ + Ant → AC ₆₀ MA	−74.0 (−73.4)	−85.6	−54
R3. C ₇₀ + Ant → AC ₇₀ MA			
<i>a</i>	−77.1 (−76.7)	−82.5	−53
<i>b</i>	−71.5	---	---
R4. IC ₆₀ MA + Ant → AIC ₆₀ BA ³			
<i>trans</i> −1	−71.6	---	---
<i>trans</i> −2 <i>a</i>	−73.1	---	---
<i>trans</i> −2 <i>b</i>	−72.8	---	---
<i>trans</i> −3 <i>a</i>	−77.1	---	---
<i>trans</i> −3 <i>b</i>	−75.9	---	---
<i>trans</i> −4 <i>a</i>	−71.2	---	---
<i>trans</i> −4 <i>b</i>	−70.7	---	---
<i>e</i> -face <i>a</i>	−77.1 (−77.1)	−82.5	−53
<i>e</i> -face <i>b</i>	−76.1	---	---
<i>e</i> -edge	−78.0	---	---
<i>cis</i> −3 <i>a</i>	−59.1	---	---
<i>cis</i> −3 <i>b</i>	−60.8	---	---
<i>cis</i> −2 <i>a</i>	−43.9	---	---
<i>cis</i> −2 <i>b</i>	−58.3	---	---

¹ The values refer to single-point energy calculations on the optimized geometries in vacuum, in parenthesis are shown the results if optimizing reactants and products in *m*-xylene solution. ² The values of $\Delta_r H_m^0$ (*m*-xylene, 298.15 K) were estimated using Equation (2). ³ The AIC₆₀BA regioisomers are ordered up-to-down by increasing proximity of Ant from Ind.

As can be observed, solvation and the correction for thermal enthalpy cause the reactions to be considerably less exothermic; the contribution of $\Delta_r H_{thermal,m}^{6-31+G(d)}$ is $\approx +10$ kJ·mol^{−1}. Given the stoichiometry of the Diels–Alder reactions, it follows that this decrease in exothermicity must come from the vibrational component. If considering the classical approximation to the translational and rotational degrees of freedom, simple calculations indicate that this vibrational contribution (ZPE + thermal) to $\Delta_r H_m^0$ (g, 298.15 K) is of about +20 kJ·mol^{−1}. This probably results from the lower frequency modes that appear in the adduct associated with single bonds and addend flipping.

Some authors have reported experimental determinations of $\Delta_r H_m^0$ for Diels–Alder reactions with C₆₀ and C₇₀ in solution [12–15]. The results from different authors vary significantly. Sarova and Berberan-Santos report a $\Delta_r H_m^0 = -81$ kJ·mol^{−1} for the reaction C₆₀ + Ant in toluene at $\langle T \rangle = 316$ K, as measured by UV-Vis spectroscopy [12]. Saunders and co-workers have studied, by NMR, the similar reactions of the two endohedral derivatives ³He@C₆₀ and ¹²⁹Xe@C₆₀ with 9,10-dimethylanthracene (DMA), determining $\Delta_r H_m^0$ values, at $\langle T \rangle \approx 310$ K, of −96 (in 1-methylnaphthalene/CD₂Cl₂) [13] and −95 kJ·mol^{−1} (in *o*-dichlorobenzene/C₆D₆) [14], respectively. In Ref. [13], the authors also determined similar $\Delta_r H_m^0$ values, under the same experimental conditions, for the reaction of C₇₀ with DMA (−88 kJ·mol^{−1}) and for the addition of a second DMA addend to C₆₀ (−94 kJ·mol^{−1}). For the reactions of endohedral H₂@C₇₀ and (H₂)₂@C₇₀ with DMA in *o*-dichlorobenzene-*d*₄ and at $\langle T \rangle = 313$ K, Murata et al. have determined by NMR the $\Delta_r H_m^0$ values of −58 and −56 kJ·mol^{−1}, respectively [15], in good agreement with our theoretical predictions.

Isomerism also has a strong impact on Diels–Alder reactions involving fullerenes. According to our computational results, AIC₆₀BA has at least five regioisomers (and four of these have an enantiomer) with important populations at equilibrium, both in the gas phase and solution. There are four *trans*-3 isomers (two enantiomeric pairs) and four equatorial isomers (*e*-face *a*, *e*-face *b*, and the enantiomer pair of *e*-edge). This gives a total of nine predominant isomers. Additionally, there are nine other residual isomers: the higher-energy *trans*-1, -2, and -4 regioisomers and their enantiomers; this excludes all *cis*-

isomers, which are practically nonexistent at equilibrium. On the other hand, IC₆₀MA and AC₆₀MA do not have isomers, and AC₇₀MA only has two meaningful isomers (*a* and *b*). Hence, the addition of the diene to the mono-adduct IC₆₀MA (R4) is entropically favored in this specific contribution of isomerism relative to the first addition to the original fullerenes (R1 to R3). However, one should not forget the contribution of molecular symmetry to entropy [45–47]. Given that C₆₀ and C₇₀ are highly symmetrical molecules and the adducts are not, symmetry can have a significant contribution to reaction thermodynamics. The impact of isomers and molecular symmetry on the thermodynamics and kinetics of fullerene reactions are currently under investigation, by experimental and computational methodologies, in our laboratory.

Although this work is focused on the thermodynamics of the fullerene reactions studied, Diels–Alder cycloadditions can be limited by kinetics. We feel that we could not conclude our discussion without a small remark on the kinetic feasibility of such reactions in the gas phase. The electrophilicity index, ω , of the reactants can be used to predict the viability of Diels–Alder reactions [48–50]. Thus, for the dienes Ind and Ant, and for the dienophiles C₆₀, C₇₀, and IC₆₀MA, we have estimated the values of ω according to the equation proposed by Parr and co-workers: $\omega = [(IP + EA)^2]/[8 \cdot (IP - EA)]$ [48], where IP and EA are, respectively, the ionization potential and the electron affinity of the molecules in the gas phase. In this context, dienophiles, being electrophilic in nature, are characterized by high ω values, while a small ω can be related to the small electrophilic tendency and thus, in principle, high nucleophilic character (as expected for dienes) [49,50]. The results are presented in Table 5. As a rough approximation, and for the sake of comparison, we also show the IP, EA, and ω values, as obtained from the HOMO and LUMO energies calculated in this work at the M06-2X/6-31+G(d) level; $IP \approx -E(\text{HOMO})$ and $EA \approx -E(\text{LUMO})$. Except for IC₆₀MA, our results show relatively good agreement with the experimental values. Most importantly, the trend in ω is the same for the two approaches: lower ω for the dienes and larger ω for the dienophiles. According to the global electrophilicity scale proposed by Domingo et al., the three fullerenes can be classified as strong electrophiles and the two dienophiles as moderate to marginal electrophiles [49,50]. Hence, this analysis provides additional theoretical support for the kinetic feasibility of the Diels–Alder reactions studied in this work.

Table 5. Reported literature values of ionization potential, IP, and electron affinities, EA, in the gas phase for the selected reactants and calculated electrophilicity index, ω . The values obtained from the HOMO and LUMO energies calculated in this work using M06-2X/6-31+G(d) are shown in parenthesis ¹.

Molecule	IP/eV	EA/eV	ω /eV
Ind	8.14 ± 0.01 [51] (7.4)	0.17 ± 0.03 [52] (−0.1)	1.1 (0.9)
Ant	7.44 ± 0.01 [53] (6.7)	0.53 ± 0.02 [54] (1.2)	1.1 (1.4)
C ₆₀	7.57 ± 0.01 [55] (7.5)	2.684 ± 0.001 [56] (3.1)	2.7 (3.1)
C ₇₀	7.36 ± 0.01 [55] (7.4)	2.76 ± 0.02 [57] (3.1)	2.8 (3.2)
IC ₆₀ MA	5.8 [58] (7.1)	3.2 [58] (2.9)	3.9 (3.0)

¹ All literature values of IP and EA were determined experimentally, except for IC₆₀MA, for which the values were determined from DFT calculations.

4. Conclusions

The calculated electronic energies of the reaction show little differentiation among the dienophiles studied (C₆₀, C₇₀, IC₆₀MA) and among the regioisomers of AIC₆₀BA (excluding the clearly unstable *cis*- isomers). Yet, for the later, the Diels–Alder reaction is energetically more favored in the order: equatorial > *trans*-3 > *trans*-2 ≈ *trans*-4 ≈ *trans*-1 > *cis*-3 > *cis*-2.

The effect of the computational method and basis set suggests the existence of stabilizing dispersive interactions between the addend and the fullerene’s surface in the adducts.

HOMA analysis revealed a significant increase in aromaticity in the four hexagons adjacent to the bond where the diene binds.

Solvation, as described by the SMD formalism, has little influence on distinguishing between dienophiles and AIC₆₀BA regioisomers.

Solvation by *m*-xylene and the contribution of thermal enthalpy decrease the exothermicity of the reactions studied by about 20 and 10 kJ·mol⁻¹, respectively.

Supplementary Materials: The following supporting information can be downloaded at: <https://www.mdpi.com/article/10.3390/org3040025/s1>. Tables S1–S3: Calculated electronic energies in vacuum and solution, and enthalpies at 298.15 K for the molecules studied; Table S4: Calculated HOMA values for the molecules studied; Table S5: Optimized geometries; Figure S1: Types of hexagons in C₇₀.

Author Contributions: Conceptualization, D.J.L.R., A.M. and C.F.R.A.C.L.; Data curation, D.J.L.R. and C.F.R.A.C.L.; Formal analysis, D.J.L.R. and C.F.R.A.C.L.; Funding acquisition, L.M.N.B.F.S. and A.M.; Investigation, D.J.L.R. and C.F.R.A.C.L.; Methodology, D.J.L.R. and C.F.R.A.C.L.; Resources, L.M.N.B.F.S. and A.M.; Software, L.M.N.B.F.S. and A.M.; Supervision, L.M.N.B.F.S. and C.F.R.A.C.L.; Writing—original draft, D.J.L.R. and C.F.R.A.C.L.; Writing—review and editing, D.J.L.R., L.M.N.B.F.S., A.M. and C.F.R.A.C.L. All authors have read and agreed to the published version of the manuscript.

Funding: The authors thank the Portuguese Foundation for Science and Technology (FCT) for financial support to the projects: CIQUP, Centro de Investigação em Química da Universidade do Porto (UIDB/00081/2020); IMS, Institute of Molecular Sciences (LA/P/0056/2020); LAQV-REQUIMTE (UIDB/50006/2020). CFRACL is financed by national funds through the FCT-I.P., in the framework of the execution of the program contract provided in paragraphs 4, 5, and 6 of art. 23 of Law no. 57/2016 of 29 August, as amended by Law no. 57/2017 of 19 July.

Data Availability Statement: Not applicable.

Conflicts of Interest: The authors declare no conflict of interest. The funders had no role in the design of the study; in the collection, analyses, or interpretation of data; in the writing of the manuscript; or in the decision to publish the results.

References

1. De La Puente, F.L.; Nierengarten, J.-F. *Fullerenes: Principles and Applications*; Royal Society of Chemistry: London, UK, 2011.
2. Taylor, R.; Walton, D.R.M. The chemistry of fullerenes. *Nature* **1993**, *363*, 685–693. [[CrossRef](#)]
3. Kroto, H.W.; Heath, J.R.; O'Brien, S.C.; Curl, R.F.; Smalley, R.E. C₆₀: Buckminsterfullerene. *Nature* **1985**, *318*, 162–163. [[CrossRef](#)]
4. Fernandez, I.; Sola, M.; Bickelhaupt, F.M. Why do cycloaddition reactions involving C₆₀ prefer [6, 6] over [5, 6] bonds? *Chem. Eur. J.* **2013**, *19*, 7416–7422. [[CrossRef](#)]
5. Olah, G.A.; Bucsi, I.; Aniszfeld, R.; Prakash, G.S. Chemical reactivity and functionalization of C₆₀ and C₇₀ fullerenes. *Carbon* **1992**, *30*, 1203–1211.
6. Yadav, B.; Kumar, R. Structure, properties and applications of fullerenes. *Int. J. Nanotechnol. Appl.* **2008**, *2*, 15–24.
7. Hirsch, A. Addition reactions of buckminsterfullerene (C₆₀). *Synthesis* **1995**, 895–913. [[CrossRef](#)]
8. Thilgen, C.; Herrmann, A.; Diederich, F. The covalent chemistry of higher fullerenes: C₇₀ and beyond. *Angew. Chem. Int. Ed.* **1997**, *36*, 2268–2280. [[CrossRef](#)]
9. Thilgen, C.; Diederich, F. The higher fullerenes: Covalent chemistry and chirality. In *Fullerenes and Related Structures*; Springer: Berlin/ Heidelberg, Germany, 1999; pp. 135–171.
10. Hirsch, A.; Lamparth, I.; Karfunkel, H.R. Fullerene chemistry in three dimensions: Isolation of seven regioisomeric bisadducts and chiral trisadducts of C₆₀ and di (ethoxycarbonyl) methylene. *Angew. Chem. Int. Ed.* **1994**, *33*, 437–438.
11. Taylor, R. Addition reactions of fullerenes. *C. R. Chim.* **2006**, *9*, 982–1000. [[CrossRef](#)]
12. Sarova, G.H.; Berberan-Santos, M.N. Kinetics of the Diels–Alder reaction between C₆₀ and acenes. *Chem. Phys. Lett.* **2004**, *397*, 402–407. [[CrossRef](#)]
13. Wang, G.W.; Saunders, M.; Cross, R.J. Reversible Diels–Alder Addition to Fullerenes: A Study of Equilibria Using ³He NMR Spectroscopy. *J. Am. Chem. Soc.* **2001**, *123*, 256–259.
14. Frunzi, M.; Cross, R.J.; Saunders, M. Effect of xenon on fullerene reactions. *J. Am. Chem. Soc.* **2007**, *129*, 13343–13346. [[CrossRef](#)] [[PubMed](#)]
15. Murata, M.; Maeda, S.; Morinaka, Y.; Murata, Y.; Komatsu, K. Synthesis and reaction of fullerene C₇₀ encapsulating two molecules of H₂. *J. Am. Chem. Soc.* **2008**, *130*, 15800–15801. [[PubMed](#)]
16. Li, Y. Fullerene-Bisadduct Acceptors for Polymer Solar Cells. *Chem. Asian J.* **2013**, *8*, 2316–2328. [[CrossRef](#)] [[PubMed](#)]

17. Yu, G.; Gao, J.; Hummelen, J.C.; Wudi, F.; Heeger, A.J. Polymer Photovoltaic Cells: Enhanced Efficiencies via a Network of Internal Donor-Acceptor Heterojunctions. *Science* **1995**, *270*, 1789–1791.
18. Qian, X.; Umari, P.; Marzari, N. First-principles investigation of organic photovoltaic materials C60, C70, [C60]PCBM, and bis-[C60]PCBM using a many-body G0W0-Lanczos approach. *Phys. Rev. B* **2015**, *91*, 245105. [[CrossRef](#)]
19. Lenes, M.; Wetzelaer, G.-J.A.H.; Kooistra, F.B.; Veenstra, S.C.; Hummelen, J.C.; Blom, P.W.M. Fullerene Bisadducts for Enhanced Open-Circuit Voltages and Efficiencies in Polymer Solar Cells. *Adv. Mater.* **2008**, *20*, 2116–2119. [[CrossRef](#)]
20. He, Y.; Chen, H.-Y.; Hou, J.; Li, Y. Indene–C60 Bisadduct: A New Acceptor for High-Performance Polymer Solar Cells. *J. Am. Chem. Soc.* **2010**, *132*, 1377–1382. [[CrossRef](#)] [[PubMed](#)]
21. He, Y.; Zhao, G.; Peng, B.; Li, Y. High-Yield Synthesis and Electrochemical and Photovoltaic Properties of Indene–C70 Bisadduct. *Adv. Funct. Mater.* **2010**, *20*, 3383–3389.
22. Chikama, A.; Fueno, H.; Fujimoto, H. Theoretical Study of the Diels–Alder Reaction of C60. Transition-State Structures and Reactivities of CC Bonds. *J. Phys. Chem.* **1995**, *99*, 8541–8549. [[CrossRef](#)]
23. Mestres, J.; Duran, M.; Sola, M. Theoretical Study of Diels–Alder Cycloadditions of Butadiene to C70. An Insight into the Chemical Reactivity of C70 as Compared to C60. *J. Phys. Chem.* **1996**, *100*, 7449–7454.
24. Umeyama, T.; Imahori, H. Isomer effects of fullerene derivatives on organic photovoltaics and perovskite solar cells. *Acc. Chem. Res.* **2019**, *52*, 2046–2055. [[CrossRef](#)]
25. Meng, X.; Zhao, G.; Xu, Q.; Tan, Z.A.; Zhang, Z.; Jiang, L.; Shu, C.; Wang, C.; Li, Y. Effects of fullerene bisadduct regioisomers on photovoltaic performance. *Adv. Funct. Mater.* **2014**, *24*, 158–163. [[CrossRef](#)]
26. Sabirov, D.S.; Terentyev, A.O.; Cataldo, F. Bisadducts of the C60 and C70 fullerenes with anthracene: Isomerism and DFT estimation of stability and polarizability. *Comput. Theor. Chem.* **2016**, *1081*, 44–48. [[CrossRef](#)]
27. Sabirov, D.S.H.; Garipova, R.R.; Bulgakov, R.G. What fullerene is more reactive toward peroxy radicals? A comparative DFT Study on ROO• addition to C60 and C70 fullerenes. *Fuller. Nanotub. Carbon Nanostruct.* **2015**, *23*, 1051–1057.
28. Ash, T.; Banerjee, S.; Debnath, T.; Das, A.K. Computational insights into the multi-Diels–Alder reactions of neutral C60 and its Li+ encapsulated analogue: A density functional theory study. *Int. J. Quantum Chem.* **2022**, *122*, e26824. [[CrossRef](#)]
29. Frisch, M.J.; Trucks, G.W.; Schlegel, H.B.; Scuseria, G.E.; Robb, M.A.; Cheeseman, J.R.; Scalmani, G.; Barone, V.; Mennucci, B.; Petersson, G.A.; et al. *Gaussian 09; Revision A.02*; Gaussian Inc.: Wallingford, CT, USA, 2009.
30. Zhao, Y.; Truhlar, D.G. The M06 suite of density functionals for main group thermochemistry, thermochemical kinetics, noncovalent interactions, excited states, and transition elements: Two new functionals and systematic testing of four M06-class functionals and 12 other functionals. *Theor. Chem. Acc.* **2008**, *120*, 215–241.
31. Josa, D.; Rodríguez-Otero, J.; Cabaleiro-Lago, E.M.; Rellán-Piñeiro, M. Analysis of the performance of DFT-D, M05-2X and M06-2X functionals for studying $\pi \cdots \pi$ interactions. *Chem. Phys. Lett.* **2013**, *557*, 170–175.
32. Denis, P.A. Theoretical investigation of the stacking interactions between curved conjugated systems and their interaction with fullerenes. *Chem. Phys. Lett.* **2011**, *516*, 82–87.
33. Marenich, A.V.; Cramer, C.J.; Truhlar, D.G. Universal solvation model based on solute electron density and on a continuum model of the solvent defined by the bulk dielectric constant and atomic surface tensions. *J. Phys. Chem. B.* **2009**, *113*, 6378–6396.
34. Kiselev, V.D.; Konovalov, A.I. Internal and external factors influencing the Diels–Alder reaction. *J. Phys. Org. Chem.* **2009**, *22*, 466–483.
35. Bühl, M.; Hirsch, A. Spherical aromaticity of fullerenes. *Chem. Rev.* **2001**, *101*, 1153–1184. [[CrossRef](#)]
36. Chen, Z.; Wu, J.I.; Corminboeuf, C.; Bohmann, J.; Lu, X.; Hirsch, A.; von Rague Schleyer, P. Is C60 buckminsterfullerene aromatic? *Phys. Chem. Chem. Phys.* **2012**, *14*, 14886–14891.
37. Krygowski, T.M. Crystallographic studies of inter- and intramolecular interactions reflected in aromatic character of π -electron systems. *J. Chem. Inf. Comput. Sci.* **1993**, *33*, 70–78.
38. Krygowski, T.M.; Cyrański, M. Separation of the energetic and geometric contributions to the aromaticity. Part IV. A general model for the π -electron systems. *Tetrahedron* **1996**, *52*, 10255–10264.
39. Krygowski, T.M.; Cyrański, M. Separation of the energetic and geometric contributions to the aromaticity of π -electron carbocyclics. *Tetrahedron* **1996**, *52*, 1713–1722.
40. Hirsch, A.; Lamparth, I.; Grösser, T.; Karfunkel, H.R. Regiochemistry of Multiple Additions to the Fullerene Core: Synthesis of a Th-Symmetric Hexakis adduct of C60 with Bis (ethoxycarbonyl) methylene. *J. Am. Chem. Soc.* **1994**, *116*, 9385–9386.
41. Lamparth, I.; Maichle-Mössmer, C.; Hirsch, A. Reversible Template-Directed Activation of Equatorial Double Bonds of the Fullerene Framework: Regioselective Direct Synthesis, Crystal Structure, and Aromatic Properties of Th-C66 (COOEt) 12. *Angew. Chem. Int. Ed. Engl.* **1995**, *34*, 1607–1609.
42. Osuna, S.; Swart, M.; Solà, M. Dispersion corrections essential for the study of chemical reactivity in fullerenes. *J. Phys. Chem. A.* **2011**, *115*, 3491–3496.
43. Osuna, S.; Morera, J.; Cases, M.; Morokuma, K.; Solà, M. Diels–Alder reaction between cyclopentadiene and C60: An analysis of the performance of the ONIOM method for the study of chemical reactivity in fullerenes and nanotubes. *J. Phys. Chem. A.* **2009**, *113*, 9721–9726.
44. Van Duijneveldt, F.B.; de Rijdt, J.G.V.D.-V.; van Lenthe, J.H. State of the art in counterpoise theory. *Chem. Rev.* **1994**, *94*, 1873–1885. [[CrossRef](#)]
45. Lin, S.K. Correlation of entropy with similarity and symmetry. *J. Chem. Inf. Comput. Sci.* **1996**, *36*, 367–376.

46. Estrada, E.; Avnir, D. Continuous symmetry numbers and entropy. *J. Am. Chem. Soc.* **2003**, *125*, 4368–4375. [[CrossRef](#)] [[PubMed](#)]
47. Pollak, E.L.I.; Pechukas, P. Symmetry numbers, not statistical factors, should be used in absolute rate theory and in Brønsted relations. *J. Am. Chem. Soc.* **1978**, *100*, 2984–2991. [[CrossRef](#)]
48. Parr, R.G.; Szentpály, L.V.; Liu, S. Electrophilicity index. *J. Am. Chem. Soc.* **1999**, *121*, 1922–1924.
49. Domingo, L.R.; Aurell, M.J.; Pérez, P.; Contreras, R. Quantitative characterization of the global electrophilicity power of common diene/dienophile pairs in Diels–Alder reactions. *Tetrahedron* **2002**, *58*, 4417–4423.
50. Domingo, L.R.; Aurell, M.J.; Pérez, P.; Contreras, R. Quantitative characterization of the local electrophilicity of organic molecules. Understanding the regioselectivity on Diels–Alder reactions. *J. Phys. Chem. A* **2002**, *106*, 6871–6875.
51. Dewar, M.J.S.; Haselbach, E.; Worley, S.D. Calculated and observed ionization potentials of unsaturated polycyclic hydro-carbons; calculated heats of formation by several semiempirical scfmo methods. *Proc. R. Soc. Lond. A* **1970**, *315*, 431–442.
52. Wojnarovits, L.; Foldiak, G. Electron capture detection of aromatic hydrocarbons. *J. Chromatogr. Sci.* **1981**, *206*, 511–519. [[CrossRef](#)]
53. Hager, J.W.; Wallace, S.C. Two-laser photoionization supersonic jet mass spectrometry of aromatic molecules. *Anal. Chem.* **1988**, *60*, 5–10.
54. Ando, N.; Mitsui, M.; Nakajima, A. Comprehensive photoelectron spectroscopic study of anionic clusters of anthracene and its alkyl derivatives: Electronic structures bridging molecules to bulk. *J. Chem. Phys.* **2007**, *127*, 234305. [[PubMed](#)]
55. Boltalina, O.V.; Ioffe, I.N.; Sidorov, L.N.; Seifert, G.; Vietze, K. Ionization energy of fullerenes. *J. Am. Chem. Soc.* **2000**, *122*, 9745–9749.
56. Huang, D.L.; Dau, P.D.; Liu, H.T.; Wang, L.S. High-resolution photoelectron imaging of cold C60(-) anions and accurate determination of the electron affinity of C60. *J. Chem. Phys.* **2014**, *140*, 224315.
57. Wang, X.B.; Woo, H.K.; Huang, X.; Kappes, M.M.; Wang, L.S. Direct experimental probe of the on-site Coulomb repulsion in the doubly charged fullerene anion C70(2-). *Phys. Rev. Lett.* **2006**, *96*, 143002. [[CrossRef](#)]
58. Nakanishi, R.; Nogimura, A.; Eguchi, R.; Kanai, K. Electronic structure of fullerene derivatives in organic photovoltaics. *Org. Electron.* **2014**, *15*, 2912–2921. [[CrossRef](#)]